Emulsion Polymerization of Styrene with Iso-Octyl-3-Mercaptopropionate as Chain Transfer Agent

R. J. Minari,[1] J. R. Vega,[1,2] M. González-Sierra,[3] G. R. Meira,[1] L. M. Gugliotta[1]

[1]INTEC (Universidad Nacional del Litoral-CONICET), Güemes 3450, 3000 Santa Fe, Argentina
[2]Facultad Regional Santa Fe (Universidad Tecnológica Nacional), Lavaisse 610, 3000 Santa Fe, Argentina
[3]IQUIOS (Universidad Nacional de Rosario - CONICET), Suipacha 531, 2000 Rosario, Argentina

ABSTRACT: Four batch and unseeded emulsion polymerizations of styrene were investigated, which included iso-octyl 3-mercaptopropionate (iOMP) as chain transfer agent (CTA). This compound was analyzed by ^{13}C NMR and GC/MS, resulting in a mixture of over 10 isomers. Because of different reactivities of the CTA isomers, the produced polystyrenes presented broad and bimodal molecular weight distributions (MWDs). A mathematical model was adjusted to the measurements, and the measured MWDs were adequately predicted when assuming the CTA as a binary mixture of high but different reactivities. © 2008 Wiley Periodicals, Inc. J Appl Polym Sci 109: 3944–3952, 2008

Key words: polystyrene; emulsion polymerization; molecular weight distribution; chain transfer agent; isooctyl 3-mercaptopropionate

INTRODUCTION

The properties of a general-purpose polystyrene (PS) are mainly determined by its molecular weight distribution (MWD). In emulsion polymerizations, chain transfer agents (CTAs) are normally required[1,2] for reducing the high molecular weights that would be otherwise produced by the ''compartmentalization'' of free radicals in the polymer particles.

Some important characteristics of CTAs used in emulsion polymerizations are their water solubility, mass transfer resistance to diffusion between phases, and ''effective'' reactivity ratios in the polymer phase $C_X = k_{fX}/k_p$, where k_{fX} is the global rate constant of chain transfer to the CTA and k_p is the global rate constant of propagation. With long hydrocarbon-chained CTAs, their concentration in the polymer phase is normally below equilibrium, and therefore the transfer reaction results in controlled diffusion.[3] However, ''effective'' C_X values are defined that assume equilibrium conditions in all phases. The mass transfer of a CTA between phases is affected by the stirring rate, the monomer-droplets size, the particle size, and the CTA diffusivity.[4,5]

The following articles have reported on the use of Cl_4C and some common mercaptans in the batch emulsion polymerization of styrene (St):[3,5–12] Table I reproduces the effective C_X ratios of some common mercaptans evaluated in the emulsion polymerization of St at 70°C. Effective C_X values close to unity induce a constant monomer to CTA ratio along the reaction, which, in turn, generate instantaneous Schulz-Flory MWDs of constant molecular weight averages along a batch process. C_X values greater than unity generate increasing molecular weights.

Different CTA isomers may exhibit quite different reactivities. This was observed in the emulsion polymerization of St and in the bulk or solution polymerizations of other monomers.[13–19] Iso-octyl 3-mercaptopropionate (iOMP) is commercialized as a mixture of several isomers, and Figure 1 presents one possible molecular structure. This compound is less odorous and toxic than other more common mercaptans such as dodecyl mercaptan. At room temperature, iOMP is a stable liquid of boiling point 112°C and density $\rho_X = 950$ g/L. Vail et al.[20] investigated the emulsion homo- and copolymerizations of methyl methacrylate (MMA) and n-butyl methacrylate (nBMA) with iOMP as CTA; observing that the polymerization rate resulted unaffected by the iOMP concentration, and that at 5% conversion the effective C_X values of MMA and nBMA were 0.4 and 1.6, respectively. Segall et al.[21] used iOMP for synthesizing a core-shell latex with a poly(benzyl methacrylate-co-styrene) core and a poly(n-butyl acrylate) shell, observing that the CTA concentration affected the particles morphology.

In the first part of this work, the composition of a commercial iOMP is analyzed by ^{13}C NMR spec-

TABLE I
Emulsion Polymerization of St at 70°C with Several Common Mercaptans: Effective Reactivity Ratios

CTA	$C_X = k_{fX}/k_p$
n-Nonyl mercaptan	1.93[7]
tert-Nonyl mercaptan	2.00[3]
n-Decyl mercaptan	4.40[9]
tert-Undecyl mercaptan	1.00[3]
n-Dodecyl mercaptan	0.69[9]
tert-Dodecyl mercaptan	0.51[3]; 0.31[7]; 1.50[9]
tert-Tridecyl mercaptan	0.29[3]

trometry and gas chromatography/mass spectrometry (GC/MS). Then, four isothermal batch emulsion-polymerizations of St with iOMP are described and interpreted in the light of a simple mathematical model. As far as the authors are aware of, this is the first article on the emulsion polymerization of St with iOMP as CTA.

CTA ANALYSIS

The used iOMP (by Aldrich Chemical, Cat. No. 55691-2, purity > 99%) is commercialized as a mixture of isomers.

The NMR spectrophotometer was a 300 MHz Brüker Avance. The ^{13}C intensities were evaluated with a standard Brüker software that included an Inverse Gated ^{1}H-decoupling sequence. Figure 2 presents the ^{13}C NMR spectrum. At least, eight different components are distinguished, characterized by the RCOO—CH_2—C_7H_{15} signals in the 60–70 ppm region. The spectrum evaluation suggested that the three-mercapto propionate group is always attached to a —CH_2— and that there is a minor contribution (≈3%) of 2′-substituted isooctyls (see Fig. 1). Thus, branching is limited to carbons C3′ or farther down the chain.

Consider the GC/MS measurements. The GC instrument was a PerkinElmer TurboMass with a WAX column (30 m in length, 0.25 mm of internal diameter, and 0.25 µm of film phase). The carrier gas was He at 1 mL/min. The temperatures in the column, injector, and detector were 150, 230, and 130°C, respectively. The samples were dissolved in hexane (1/200 by weight) and injected in a split injection mode. Figures 3 and 4 represent the GC-chromatogram and the MS spectra of the five most abundant components. The chromatogram suggests a mixture of 10 or more isomers, with the five more abundant components representing more than 95% of the total mass (Fig. 3). However, the most abundant ''component'' (of mass fraction 49.7%) consists of two overlapped peaks that possibly correspond to an isomers mixture. Figure 4 shows the MS spectra of isooctyl 3-mercaptopropionates. Although the

peaks at M/e = 218 correspond to the molecular ion, the peaks at 119, 71/70/69, and 57 correspond to the isomer ion series. The observed variations are mainly in the relative signal intensities; and this made the direct structure assignment difficult.

All the mentioned results confirm that the product is a mixture of isomers of $M_X = 218.3$ g/mol. Unfortunately, the observed components may correspond to more than one associated isomer, thus making it impossible to determine the mass fraction of each possible isomer. However, it is hoped that most of the isomers were effectively fractionated by GC. By neglecting the less abundant isomers and assuming the CTA as mixture of the five most abundant components, Table II presents their relative mass fractions and retention times.

Apart from the analytical measurements, the water solubility of iOMP was measured to estimate its partition coefficient between the monomer-droplets phase and the aqueous phase. The solubility was determined from a saturated iOMP solution, using a total organic carbon (TOC) analyzer by Shimadzu (TOC-5000A). The measurement included the inorganic carbon of the dissolved CO_2. The saturated solutions were prepared by first dispersing 0.5 g of iOMP in 0.3 L of water and then separating the non-dissolved CTA droplets by multiple extraction centrifugation at 5000 rpm. Bearing in mind the iOMP carbon content of 132.15 g/mol, a water solubility of 5.67×10^{-5} mol/L was determined from the TOC measurement ($=7.49 \times 10^{-3}$ g/L). Clearly, the obtained solubility cannot distinguish between the different isomers.

POLYMERIZATION EXPERIMENTS

Four batch polymerizations were carried out at 70°C in a 1-L glass reactor. The reactor included a modified anchor stirrer, a sampling system, and a N_2 inlet. The temperature was controlled by means of a digital thermometer and a thermostatic bath. The stirring rate was 250 rpm.

Distilled and deionized (DDI) water was used throughout the work. The following reagents were used as received: sodium lauryl sulfate emulsifier (Mallinckrodt, 95% purity); $K_2S_2O_8$ initiator (Mallinckrodt, 99% purity); $NaCO_3H$ buffer salt (Anedra, purity 99.7%); and iOMP CTA (Aldrich, purity > 99%). The monomer (commercial grade St from
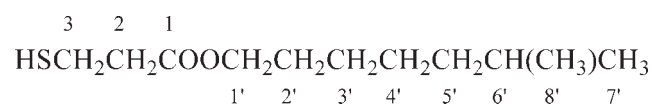
$$\overset{3 \quad \ 2 \quad \ \ 1}{HSCH_2CH_2COOCH_2CH_2CH_2CH_2CH_2CH(CH_3)CH_3}$$
$$\underset{1' \quad \ 2' \quad \ 3' \quad \ 4' \quad \ 5' \quad \ 6' \ \ 8' \quad \ 7'}{}$$

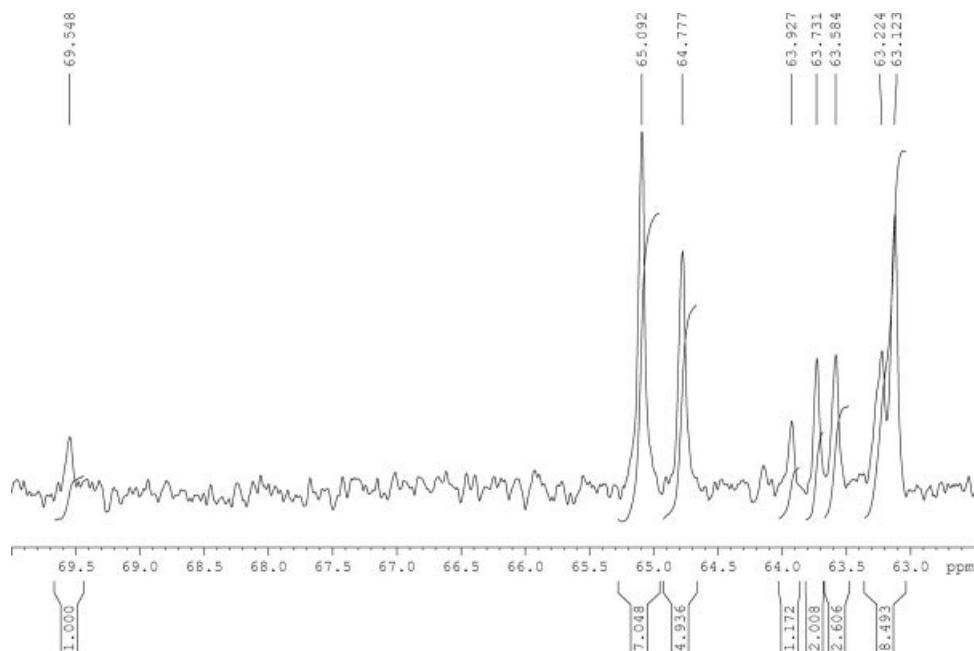**Figure 1** A possible structure of isooctyl 3-mercaptopropionate (iOMP).

Figure 2 ^{13}C NMR analysis of the iOMP mixture: expanded 70–60 ppm region.

Petrobras Energía S.A., Argentina) was first washed several times with a 15% KOH solution, then washed with DDI water until neutral pH, and finally dried with $CaCl_2$.

The recipes are in the upper section of Table III. Except for CTA, they closely reproduce the recipes and conditions in Salazar et al.[7] and Gugliotta et al.[22]; and, therefore, most of the model parameters were directly adopted from such publications. The reactions involved a constant temperature but varying amounts of CTA; with Exp. 4 carried out in the absence of CTA. The polymerizations were as follows. First, the emulsifier and buffer salt were dissolved in 500 g of water and loaded into the reactor. Then, the monomer and the CTA were loaded, and the temperature was stabilized at 70°C. Finally, the

Figure 3 GC chromatogram of the iOMP mixture. The numbers indicate the absolute mass fractions of the five most abundant isomers; and t_r represents retention time.

initiator was dissolved in the remaining water (10 g), and the solution was loaded into the reactor to start the polymerization. The reactions were carried out under continuous N_2 bubbling. Samples were withdrawn during the reactions, and the following was measured: (i) total monomer conversion x, by gravimetry; (ii) unswollen average particle diameter $\bar{d}_p$, with a Brookhaven BI-9000 AT dynamic light scattering photometer; and (iii) MWD and their averages, with a Waters 1515 size exclusion chromatograph (SEC) fitted with a differential refractometer (Waters 2414) and a set of six μ-styragel Waters columns, of nominal fractionation range 10^2–10^7 g/mol. The molecular weights were determined from a direct calibration with narrow PS standards in the range 10^3–10^6 g/mol. The very high molecular weights observed in Exp. 4 saturated the SEC columns, and therefore global measurements of $\bar{M}_v$ were implemented at room temperature with tetrahydrofuran as solvent. The glass capillary viscometer (of inner diameter 0.44 mm) was fitted in an automatic meniscus detector (Schott Geräte AVS 300). The required Mark-Houwink constants ($a = 0.755$; and $K = 8.965 \times 10^{-5}$ dL/g) were determined with the same offline viscometer and the mentioned set of PS standards.

Figure 5 represents the measurements of x, $\bar{d}_p$, $\bar{M}_n$, $\bar{M}_w$, and $\bar{M}_v$ (in symbols); and Table III presents the same variables for the samples taken at 30 and 150 min. For Exps. 1–3, Figure 6 represents the MWD measurements at four different conversions (in continuous trace). Figure 5(a,b) shows that the CTA concentration exhibits a minor effect on the monomer
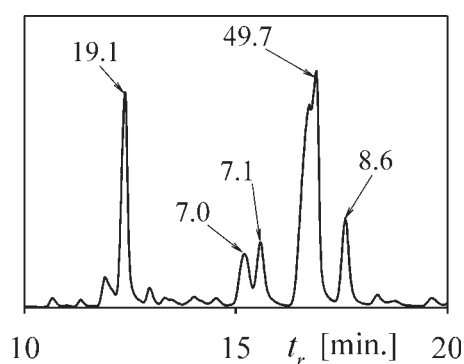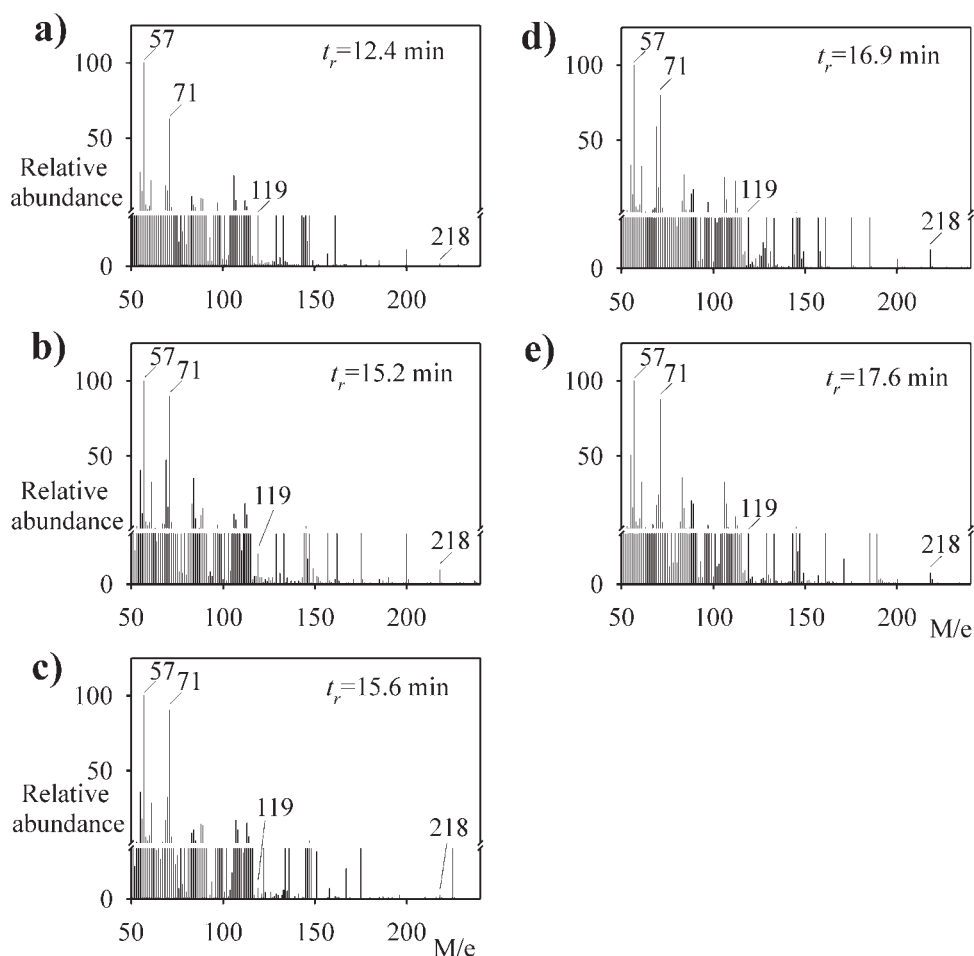
Figure 4 MS of the five most abundant iOMP components of Figure 3. M/e represents the ion mass to charge ratio.

conversion and average particle diameter. Thus, the initial rate of polymerization seems to increase with the CTA concentration, and a small induction period is observed in Exp. 4 without CTA [Fig. 5(a)]. The increase of the polymerization rate could be explained by an increase in the particle nucleation rate by desorption of CTA radicals from the polymer particles followed by absorption into the emulsifier micelles.

As expected, the iOMP concentration considerably affects the average molecular weights [Fig. 5(c,d)]. In Exps. 1–3, the average molecular weights are increased along the reactions; indicating "effective" C_X values larger than unity. In the absence of CTA (Exp. 4), $\bar{M}_v$ remains essentially constant, and this suggests a molecular weights control by chain transfer to the monomer.

The MWDs are initially relatively narrow and symmetrical, but become increasingly broader and bimodal at higher conversions (Fig. 6). Such bimodalities suggest large differences in the reactivities of the various iOMP isomers.

TABLE II
GC/MS Analysis of iOMP: Retention Times and Mass Fractions of the Five More Abundant Components

Component	t_r (min)	Mass fractions (%)[a]
X_1	12.4	25.4
X_2	15.2	7.8
X_3	15.6	7.8
X_4	16.9	50.1
X_5	17.6	8.9

[a] The less abundant components are neglected.

MATHEMATICAL MODEL AND SIMULATION RESULTS

The mathematical model is partially presented in the Appendix. It is based on the model by Salazar et al.,[7] but it was extended to the case of a CTA mixture. The kinetic mechanism considers: (i) initiation, propagation, and recombination termination in the aqueous phase; and (ii) propagation, chain transfer to the CTA, chain transfer to the monomer, and recombination termination in the polymer phase (see

TABLE III
Batch Emulsion Polymerizations of St carried out at 70°C: Recipes and Measurements at 30 and 150 min

	Exp. 1	Exp. 2	Exp. 3	Exp. 4
Initial reagent concentrations in pphm[a]				
St	100	100	100	100
iOMP	1.15	1.02	0.63	0
Initiator[b]	0.181	0.180	0.180	0.179
Emulsifier[c]	2.00	2.03	2.00	2.00
Buffer[d]	0.180	0.151	0.182	0.181
Water	397.4	397.9	395.7	395.6
Sample at 30 min				
x (%)	**69.8** (70.1)	**65.5** (69.9)	**58.9** (62.7)	**59.3** (60.4)
$\bar{d}_p$ (nm)	**83.7** (80.5)	**85.9** (80.7)	**81.9** (82.3)	**80.5** (83.0)
$\bar{M}_n$ (g/mol)	**12,800** (13,300)	**14,700** (15,000)	**27,600** (21,900)	**−**(890,500)
$\bar{M}_w$ (g/mol)	**120,000** (91,500)	**77,200** (101,000)	**145,300** (131,300)	**−**(1,781,000)
$\bar{M}_w/\bar{M}_n$ (−)	**9.4** (6.9)	**5.3** (6.7)	**5.3** (6.0)	**−**(2.0)
$\bar{M}_v$ (g/mol)	**78,200**[e] (78,700)	**67,800**[e] (87,000)	**124,100**[e] (113,700)	**1,730,600**[f] (1,680,400)
Final sample at 150 min				
x (%)	**97.7** (99.9)	**98.3** (99.7)	**98.2** (99.8)	**97.7** (99.9)
$\bar{d}_p$ (nm)	**90.7** (89.9)	**96.1** (90.4)	**89.7** (96.0)	**90.8** (98.1)
$\bar{M}_n$ (g/mol)	**22,400** (18,500)	**26,600** (21,000)	**54,700** (33,300)	**−**(890,500)
$\bar{M}_w$ (g/mol)	**167,000** (260,300)	**168,900** (280,600)	**402,100** (366,700)	**−**(1,781,000)
$\bar{M}_w/\bar{M}_n$ (−)	**7.4** (14.0)	**6.3** (13.4)	**7.3** (11.0)	**−**(2.0)
$\bar{M}_v$ (g/mol)	**150,400**[e] (198,600)	**159,300**[e] (215,600)	**301,100**[e] (288,400)	**1,529,800**[f] (1,680,400)

The measurements are in bold font, and the model predictions are in parentheses.
[a] Parts per hundred monomer.
[b] $K_2S_2O_8$.
[c] Sodium lauryl sulfate.
[d] $NaCO_3H$.
[e] Estimated by SEC.
[f] Estimated by capillary viscometry.

Appendix). The main model hypotheses are (a) the polymer particles are generated by micellar nucleation; (b) pseudo-steady state for the free-radicals in both the aqueous and polymer phases; (c) the monomer is only consumed in the polymer phase by propagation (long-chain hypothesis); (d) monodis-
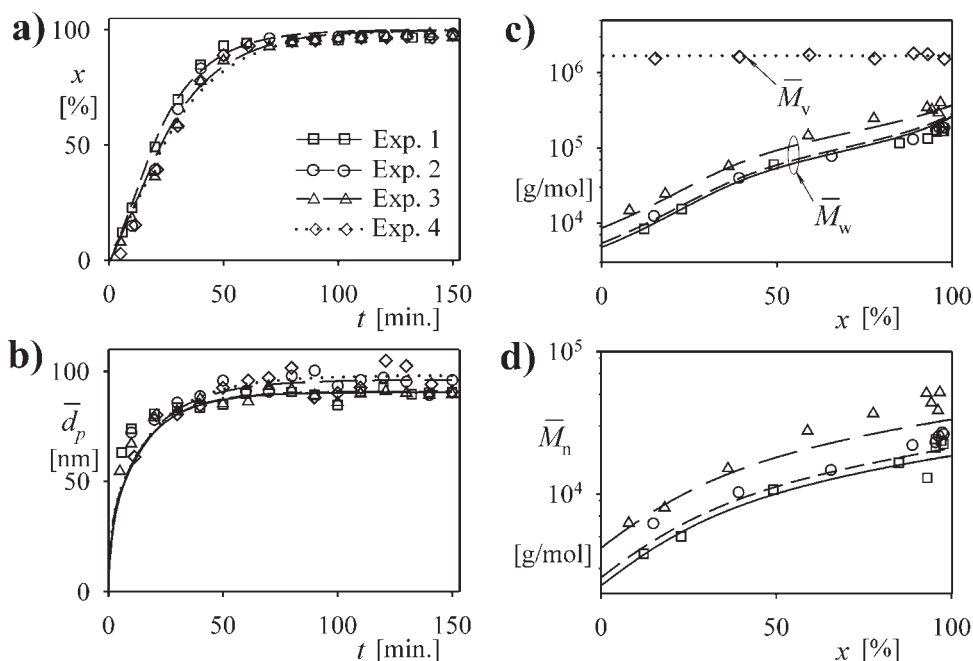

Figure 5 Experiments 1–4: (a) monomer conversion (x); (b) average particle diameter ($\bar{d}_p$); and (c–e) average molecular weights ($\bar{M}_w$, $\bar{M}_n$, and $\bar{M}_v$). The measurements are indicated by symbols and the model predictions by traces.
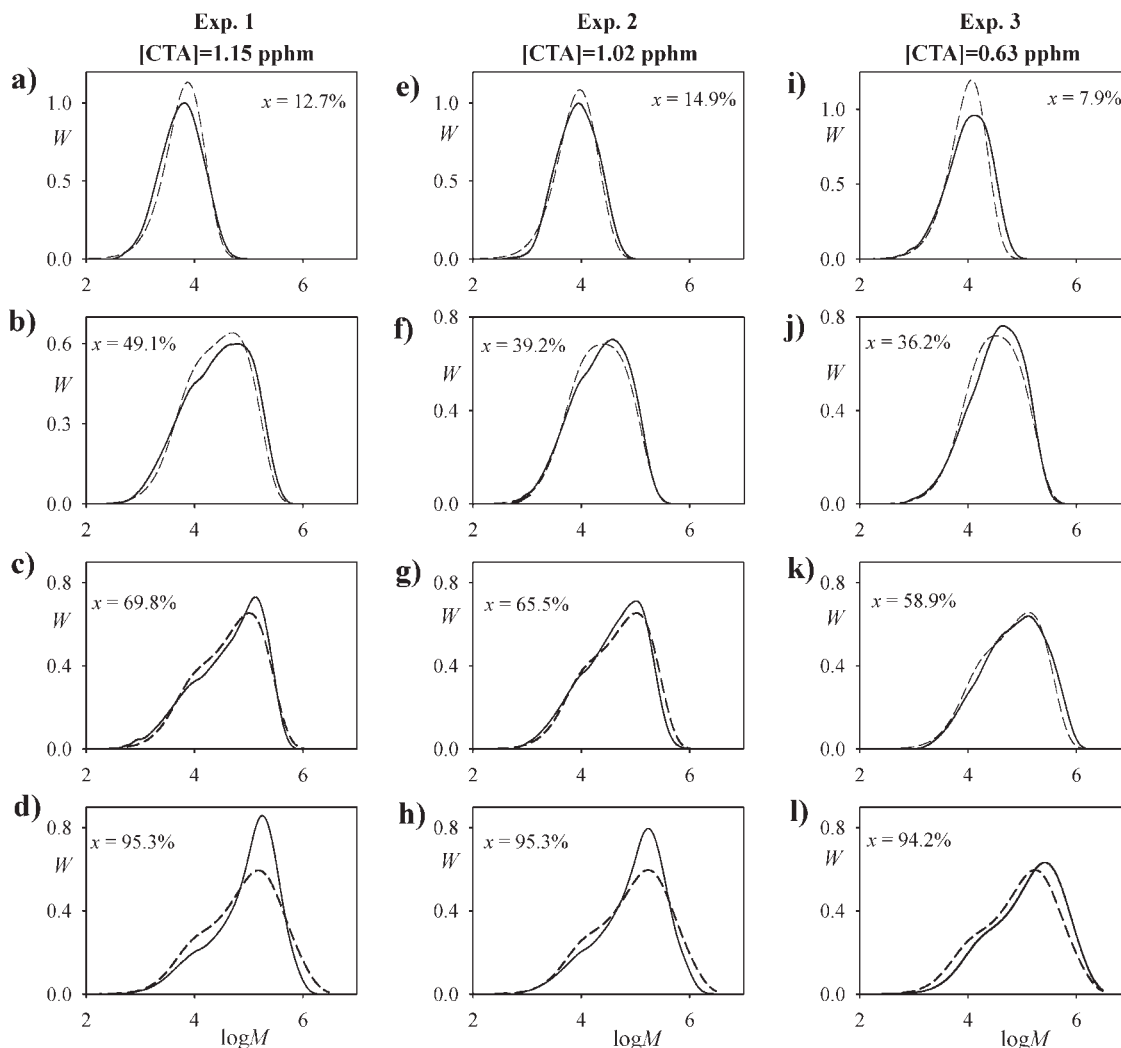
Figure 6 Measured and predicted MWDs for Exp. 1 (a–d), Exp. 2 (e–h), and Exp. 3 (i–l). The measurements are indicated by continuous traces and the model predictions by dashed traces.

perse particle size distribution; (e) desorption of primary CTA radicals from the polymer particles, with a global desorption coefficient calculated as in Nomura et al.[25]; (f) the monomer and the CTA are distributed between the phases according to equilibrium, with constant partition coefficients; (g) all CTA isomers are equally distributed between the phases; and (h) the instantaneous MWD is calculated assuming a pseudo-bulk polymerization controlled by chain transfer to the monomer and to the CTA.

The model parameters are presented in Table IV. Except for those related to the CTA, most of the parameters were directly taken from Salazar et al.[7] Consider the estimation of the CTA partition coefficient between the monomer droplets phase (d) and the aqueous phase (w), defined by $K_{Xdw} \equiv [X]_d/[X]_w$. This coefficient was calculated under saturation conditions. On one hand, the droplets phase are considered as pure CTA, yielding $[X]_d = \rho_X/M_X = 4.35$ mol/L. On the other hand, $[X]_w$ was adopted as the

water solubility determined by the TOC measurement, that is, $[X]_w = 5.67 \times 10^{-5}$ mol/L. By substituting the previous values, it results $K_{Xdw} = 7.67 \times 10^4$. The CTA partition coefficient between the aqueous phase and the polymer particles phase (p) K_{Xwp} was estimated as in Nomura et al.,[25] who observed that for emulsion polymerizations of St with linear mercaptans containing between 7 and 12 carbon atoms, the CTA and the monomer are identically distributed between the monomer droplets and the polymer particles, that is, $K_{Xdw} K_{Xwp} \cong K_{Stdw} K_{Stwp}$. By replacing into this expression, the previous value of K_{Xdw} and the values of K_{Stdw} and K_{Stwp} presented in Table IV, one obtains: $K_{Xwp} = 2.19 \times 10^{-5}$ (Table IV).

The rate constants of chain transfer to the monomer and to the different CTA components (k_{fM} and k_{fX}, respectively), and the ratio between the mass transfer resistance of iOMP radicals on the water side and the overall mass transfer resistance (δ) were adjusted through an iterative procedure that mini-

TABLE IV
Model Parameters for the Batch Emulsion Polymerization of St with iOMP at 70°C

Parameter	Value	Reference
D_{Xw}	8.75×10^{-6} dm^2 min^{-1}	Wilke-Chang correlation[26]
δ	1.61×10^{-4}	Adjusted in this work
k_d[a]	1.30×10^{-3} min^{-1}	Salazar et al.[7]
k_p[b]	2.41×10^{4} dm^3 mol^{-1} min^{-1}	Salazar et al.[7]
k_{tp}[c]	2.88×10^{7} dm^3 mol^{-1} min^{-1}	Salazar et al.[7]
k_{tw}[d]	8.40×10^{9} dm^3 mol^{-1} min^{-1}	Salazar et al.[7]
K_{Stdw}	1.81×10^{3}	Salazar et al.[7]
K_{Stwp}	9.26×10^{-4}	Salazar et al.[7]
K_{Xdw}	7.67×10^{4}	Determined in this work
K_{Xwp}	2.19×10^{-5}	Determined in this work
k_{fM}	2.84 dm^3 mol^{-1} min^{-1}	Adjusted in this work
a[e]	0.755	Determined in this work
k_{fX_1}	4.50×10^{4} dm^3 mol^{-1} min^{-1}	Adjusted in this work
k_{fX_m}	25.0×10^{4} dm^3 mol^{-1} min^{-1}	Adjusted in this work

[a] Initiator decomposition rate constant.
[b] Propagation rate constant.
[c] Termination rate constant in polymer phase.
[d] Termination rate constant in aqueous phase.
[e] Mark-Houwink exponent used in eq. (A16).

mized the average errors between measurements and model predictions. First, the δ parameter was adjusted to the time evolutions of conversion [Fig. 5(a)]. Then, k_{fM} was adjusted to the (essentially constant) values of $\bar{M}_v$ of Exp. 4 without CTA. Finally, the k_{fX_i} values were adjusted to the evolutions of $\bar{M}_n$ and $\bar{M}_w$ of Exps. 1–3. When assuming the CTA as a mixture of five components, the chain transfer constant of isomer X_1 (of mass fraction 25.4%) resulted: $k_{fX_1} = 4.50 \times 10^4$ dm^3 mol^{-1} min^{-1}, whereas all the other constants ranged between 18.7×10^4 and 22.7×10^4 dm^3 mol^{-1} min^{-1} (i.e., they were all quite similar to each other and about five times lower than k_{fX_1}). This suggested to reconsider the CTA as a binary mixture, with a component X_1 (of mass fraction 25.4%) and a hypothetical second component X_m (of mass fraction 74.6%). The corresponding reactivities resulted $k_{fX_1} = 4.50 \times 10^4$ dm^3 mol^{-1} min^{-1} and $k_{fX_m} = 25.0 \times 10^4$ dm^3 mol^{-1} min^{-1} (see bottom of Table IV), yielding $C_{X_1} \cong 1.87$, and $C_{X_m} \cong 10.4$.

The model predictions are in Figure 5, Table III, and Figure 6. In all cases, relatively small differences between measurements and model predictions are observed. For Exp. 2, some additional model predictions are presented in Figure 7. Figure 7(a) shows the concentrations of St, X_1, and X_m in the polymer phase. The monomer concentration remains essentially constant, whereas the monomer droplets phase is still present (up to $x \sim 50\%$); and then it monotonically decreases. Also, X_m is rapidly consumed whereas X_1 remains throughout the reaction. To help interpret the cumulative MWDs of Figure 6(e–h), Figure 7(b) shows the instantaneous Schulz-Flory MWDs produced at the four analyzed conversions; and Figure 7(c) shows the corresponding global τ
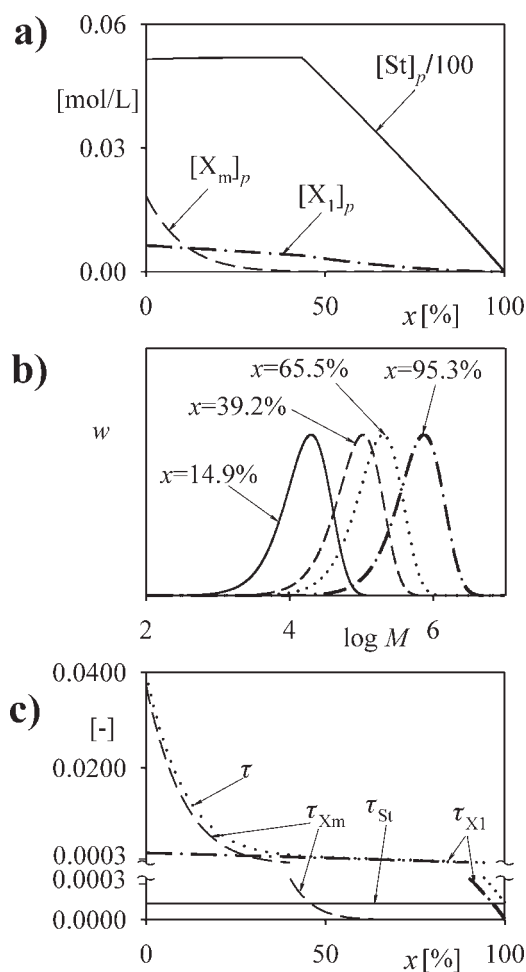

Figure 7 Experiment 2. Model predictions for (a) concentrations of St, X_1, and X_m; (b) instantaneous MWDs produced at 14.9, 65.5, and 95.3% conversion; and (c) total Schulz-Flory parameter τ, and individual components τ_{X1}, τ_{Xm}, and τ_{St}.

parameter and its components: $\tau_{X_1} = k_{fX_1}[X_1]_p/k_p[St]_p$; $\tau_{X_m} = k_{fX_m}[X_m]_p/k_p[St]_p$; and $\tau_{St} = k_{fM}/k_p$ [see eq. (A12)]. Note that two different scales are used in the ordinates of Figure 7(c). Initially, the instantaneous MWDs are controlled by chain transfer to the highly reactive X_m, producing a low molar mass material of a narrow distribution [Fig. 7(b)]. At intermediate conversions, X_m is mostly consumed, and the slower X_1 produces a higher molar mass material [Fig. 7(b)]. At the end of the polymerization, X_1 is also essentially consumed, and all the dead polymers are generated by chain transfer to the monomer.
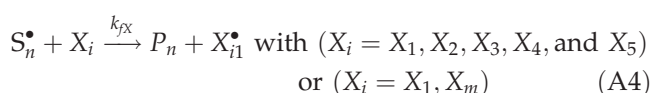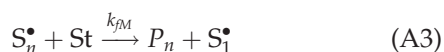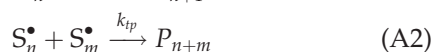
CONCLUSIONS

In the emulsion polymerization of St, the iOMP concentration exhibits a moderate effect on the monomer conversion and particle diameters, but a large effect on the MWDs. The CTA is a mixture of more than 10 isomers, with five of them constituting more than 95% of the total mass; and four of such five exhibiting similar chain-transfer characteristics. This suggested to assume the iOMP mixture as binary, with a slower X_1 component of mass fraction 25%, and a faster X_m component of mass fraction 75%. Although the ''effective'' C_X ratio of X_1 is similar to that of other more common mercaptans (Table I), the C_X value of X_m is about five times larger. Even though high-CTA reactivities are, in principle, useful for controlling the molecular weights, the different (and high) reactivities of X_1 and X_m generate broad and bimodal MWDs in batch processes at high conversions. This problem could be overcome with semibatch additions of the CTA or using intermediate additions in continuous stirred reactor trains. In a future communication, a policy for producing PS of prespecified polydispersity values will be presented, which is based on semibatch additions of iOMP along the reaction.

APPENDIX: MATHEMATICAL MODEL

The following kinetic scheme is adopted in the polymer phase, where the MWD is developed[7]:

$$S_n^\bullet + St \xrightarrow{k_p} S_{n+1}^\bullet \tag{A1}$$

$$S_n^\bullet + S_m^\bullet \xrightarrow{k_{tp}} P_{n+m} \tag{A2}$$

$$S_n^\bullet + St \xrightarrow{k_{fM}} P_n + S_1^\bullet \tag{A3}$$

$$S_n^\bullet + X_i \xrightarrow{k_{fX}} P_n + X_{i1}^\bullet \text{ with } (X_i = X_1, X_2, X_3, X_4, \text{and } X_5)$$
$$\text{or } (X_i = X_1, X_m) \tag{A4}$$

where X_i are the iOMP isomers (of molar mass 218.3 g/mol). The termination reaction (A2) is considered in the calculation of the monomer conversion, but it is neglected in the calculation of the MWD.

The molar balances for St (N_{St}) and for a generic X_i (N_{X_i}); together with the balance of polymer particles (N_p) result[7]:

$$\frac{dN_{St}}{dt} = -k_p[St]_p \frac{\bar{n}N_p}{N_A} \tag{A5}$$

$$\frac{dN_{Xi}}{dt} = -k_{fX_i}[X_i]_p \frac{\bar{n}N_p}{N_A} \quad (i = 1,2,3,4,5, \text{and } m) \tag{A6}$$

$$\frac{dN_p}{dt} = \frac{A_m}{A_m + A_p}\left(2fk_d[I]_w + k_{de}\frac{\bar{n}N_p}{N_A V_w} - k_{tw}[R^\bullet]_w^2\right)V_w N_A \tag{A7}$$

where k_p and k_{fX_i} are the rate constants of propagation and chain transfer to X_i, respectively, $[j]_p$ is the concentration of j ($=St$ or X_i) in the polymer particles, $\bar{n}$ is the average number of radicals per particle, N_A is the Avogadro's constant, A_m and A_p are the surface areas of micelles and polymer particles, respectively, f is the initiator efficiency, k_d is the rate constant of initiation, $[I]_w$ is the concentration of initiator in the aqueous phase, k_{de} is the rate constant of desorption of X_i radicals from the polymer particles, k_{tw} is the termination rate constant of free radicals in the aqueous phase, $[R^\bullet]_w$ is the concentration of free radicals in the aqueous phase, and V_w is the total aqueous phase volume.

Assuming equilibrium between phases for the monomer and the CTA with constant partition coefficients, the concentrations of such components in the polymer particles are

$$[j]_p = \frac{N_j}{K_{jdw}K_{jwp}V_d + K_{jwp}V_w + V_p} \quad (j = St, X_i) \tag{A8}$$

where V_d and V_p are the phase volumes of monomer droplets and polymer particles.

The global volumes of monomer droplets, polymer particles, and aqueous phase were obtained from their corresponding volume balances.[7] The polymer particles area and the average particle diameter ($\bar{d}_p$) were calculated from the polymer phase volume and N_p. The micelles area was calculated from the emulsifier concentration and its characteristics.[7]

In the aqueous phase, the total concentration of free radicals $[R^\bullet]_w$ was calculated from a global-free radicals balance.[7] In the polymer phase, $\bar{n}$ was calculated from the classical expression by Ugelstad and

Hansen[23], which includes a rate constant of radical desorption from the polymer particles k_{de}, given by[24]:

$$k_{de} = \frac{12 D_{Xw} \delta \sum_{X_i} \left(k_{fX_i}[X_i]_p \right) K_{X_{wp}}}{\bar{d}_p^2 k_p [St]_p} \quad (A9)$$

where D_{Xw} is the diffusion coefficient of CTA radicals in the aqueous phase and δ is the ratio between the mass transfer resistance of CTA radicals in the water side and the overall mass transfer resistance.

The monomer conversion (x) was calculated from

$$x = \frac{N_{St}^0 - N_S}{N_{St}^0} \quad (A10)$$

where N_{St}^0 are the initial St moles.

The instantaneously produced polymer exhibits a normalized Schulz-Flory MWD $w(M)$ represented by

$$w(M) = \frac{M\tau^2}{M_{St}^2} \exp\left(-\frac{M\tau}{M_{St}}\right) \quad (A11)$$

where M_{St} is the styrene molecular weight and τ is a dimensionless parameter given by

$$\tau = \frac{\sum_{X_i} k_{fX_i}[X_i]_p}{k_p[St]_p} + \frac{k_{fM}}{k_p} = \sum_{X_i} \tau_{X_i} + \tau_{St} \quad (A12)$$

At any conversion, the cumulative MWD $W(M, x)$ is calculated from

$$W(M) = N_{St}^0 M_{St} \int w(M) dx \quad (A13)$$

Finally, the average molecular weights are obtained from

$$\bar{M}_n = \frac{\int W(M) dM}{\int W(M)/M \, dM} \quad (A14)$$

$$\bar{M}_w = \frac{\int W(M) M \, dM}{\int W(M) \, dM} \quad (A15)$$

$$\bar{M}_v = \left(\frac{\int W(M) M^a \, dM}{\int W(M) \, dM} \right)^{1/a} \quad (A16)$$

where a is the Mark-Houwink constant at the viscosity measurement conditions.

References

1. Lichti, G.; Gilbert, R.G.; Napper D. H. In Emulsion Polymerization; Piirma, I., Ed.; Academic Press: New York 1982; p 93–114.
2. Gilbert, R. G. Emulsion Polymerization. A Mechanistic Approach. Academic Press: London, 1995.
3. Harelle, L.; Pith, T.; Hu, G.; Lambla, M. J Appl Polym Sci 1994, 52, 1105.
4. Zubitur, M.; Mendoza, J.; de la Cal, J. C.; Asua, J. M. Macromol Symp 2000, 150, 13.
5. Cunningham, M. F.; Witty, T. Polym React Eng 2003, 11, 519.
6. Echevarría, A.; Leiza, J. R.; de la Cal, J. C.; Asua, J. M. AIChE J 1998, 44, 1667.
7. Salazar, A.; Gugliotta, L. M.; Vega, J. R.; Meira, G. R. Ind Eng Chem Res 1998, 37, 3582.
8. Mendoza, J.; de la Cal, J. C.; Asua, J. M. J Polym Sci Part A: Polym Chem 2000, 38, 4490.
9. Dietrich, B. K.; Pryor, W. A.; Wu, S. J. J Appl Polym Sci 1988, 36, 1129.
10. Uraneck, C. A.; Burleigh, J. E. J Appl Polym Sci 1970, 14, 267.
11. Cunningham, M. F.; Ma, J. W. J Appl Polym Sci 2000, 78, 217.
12. Ma, J. W.; Cunningham, M. F. Macromol Symp 2000, 150, 85.
13. Brandrup, J.; Immergut, E. H.; Grulke, E. A. Polymer Handbook, 4th ed.; Wiley: New York, 1999; Chapter II.
14. Dinaburg, V. A.; Vansheidt, A. A. Zh Obshch Khim 1954, 24, 840.
15. Kaeriyama, K. Nippon Kagaku Zasshi 1976, 88, 783.
16. Minoura, Y.; Sugimura, T. J Polym Sci A-1 1966, 4, 2721.
17. Barton, S. C.; Bird, R. A.; Ruseel, K. E. Can J Chem 1963, 41, 2737.
18. Meehan, E. J.; Kolthoff, I. M.; Sinha, P. R. J Polym Sci 1955, 16, 471.
19. Mortimer, G. A. J Polym Sci A-1 1972, 10, 163.
20. Vail, N. K.; Barlow, J. W.; Beaman, J. J.; Marcus, H. L.; Bourell, D. L. J Appl Polym Sci 1994, 52, 789.
21. Segall, I.; Diminie, V. L.; El-Aaseer, M. S.; Spskey, P. R.; Mylonakis, S. G. J Appl Polym Sci 1995, 58, 401.
22. Gugliotta, L. M.; Salazar, A.; Vega, J. R.; Meira, G. R. Polymer 2001, 42, 2719.
23. Ugelstad, J.; Hasen, F. K. Rubber Chem Technol 1976, 49, 736.
24. Nomura, M.; Minamino, Y.; Fujita, K. J Polym Sci Polym Chem 1982, 20, 1261.
25. Nomura, M.; Suzuki, H.; Tokunaga, H.; Fujita, K. J Appl Polym Sci 1994, 51, 21.
26. Wilke, C. R.; Chang, P. C. AIChE J 1955, 1, 264.